A Cell-Based Screening Identifies Compounds from the Stem of *Momordica charantia* that Overcome Insulin Resistance and Activate AMP-Activated Protein Kinase

HSUEH-LING CHENG,*,† HSIN-KAI HUANG,† CHI-I CHANG,† CHUNG-PAO TSAI,†
AND CHANG-HUNG CHOU*,‡

Graduate Institute of Biotechnology, National Pingtung University of Science and Technology,
Pingtung, Taiwan 91201, Research Center for Biodiversity, China Medical University,
Taichung, Taiwan 40402

Treatment of insulin resistance is a critical strategy in the prevention and management of type 2 diabetes. The crude extracts from all parts of *Momordica charantia* L. have been reported by many studies for the effective treatment of diabetes and related complications. However, the exact ingredients responsible for the hypoglycemic effect and the underlying mechanism of their actions have not been well characterized because of the lack of a proper assay and screening system. A new cell-based, nonradioactive, and nonfluorescent screening method was demonstrated in this study to screen for natural products from the stem of *M. charantia*, aiming to identify hypoglycemic components that can overcome cellular insulin resistance. The results suggest triterpenoids being potential hypoglycemic components of the plant and the mechanism underlying their action involving AMP-activated protein kinase.

INTRODUCTION

The occurrence of type 2 diabetes is closely associated with the development of insulin resistance, followed by the progressive decline of pancreatic β-cell function that results in insufficient insulin secretion. This eventually leads to overt diabetic phenomena of hyperglycemia and dyslipidaemia (*1*). Insulin resistance is the inability of insulin-responsive tissues, mainly liver, muscles, and adipose tissues, to respond normally to circulating insulin. Treatment of insulin resistance is a major strategy in the prevention and management of type 2 diabetes (*2, 3*). Moreover, insulin resistance is also linked to other common health problems, including obesity, hypertension, atherosclerosis, and hepatic steatosis (*4, 5*), and so forth. Hence, the worldwide prevalence of diabetes and insulin resistance has provoked the study and search for therapeutic agents.

Plants and herbal preparations have been used as alternative therapy. *Momordica charantia* L., belonging to the Cucurbitaceae family, also known as bitter gourd or bitter melon, has been widely consumed as a vegetable as well as herbal medicine,

particularly for diabetic patients, in India, South America, and Asia (*6–8*). The crude extract from either the fruit, seed, foliage, or whole plant of *M. charantia* has been reported effective by many studies in the treatment of diabetes and related complications in animal models (*6*). There was sporadic isolation of some natural products from *M. charantia* that were suggested for hypoglycemic activities in experimental animals (*9–11*). However, the exact ingredients of *M. charantia* responsible for the hypoglycemic effect and the underlying molecular mechanisms of their actions, have not been systematically investigated because of the lack of an appropriate assay and screening system.

The low-throughput property of animal tests limits their application for the screening of bioactive compounds from complicated sources. Therefore, *in vitro* models using cell culture designed to mimic specific physiological events occurring at the cellular and subcellular levels provide an attractive alternative for high throughput assays. Normal muscle and adipose cell lines, such as C2C12 cells and 3T3-L1 cells, respectively, are very often used as *in vitro* models for testing the effects of antidiabetic agents (*12–14*). However, these cell lines need to be differentiated before tests to acquire insulin sensitivity, which increases the operation complexity and limits the throughput of these cell lines as screening systems. Moreover, the extent of cell differentiation may be different between operations and dishes, leading to unequal insulin

* Corresponding author. (C.-H.C.) Phone: 886-4-2205-3366 ext. 1633. Fax: 886-4-2207-1500. E-mail: choumasa@mail.cmu.edu.tw. (H.-L.C.) Phone: 886-8-7703202 ext. 5186. Fax: 886-8-7740550. E-mail: hlcheng@mail.npust.edu.tw.
† National Pingtung University of Science and Technology.
‡ China Medical University.

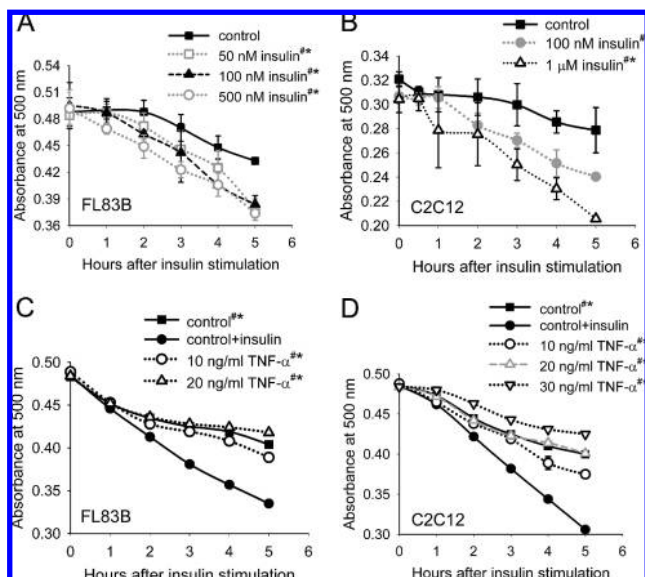**6836** *J. Agric. Food Chem.,* Vol. 56, No. 16, 2008

Cheng et al.

Figure 1. Insulin sensitivity and induction of insulin resistance of FL83B cells and C2C12 cells. In **A** and **B**, the insulin sensitivity of FL83B cells (**A**) and differentiated C2C12 cells (**B**) were characterized. Control was cells without insulin stimulation; other groups of cells were stimulated with either 50 nM, 100 nM, 500 nM, or 1 μM of insulin, as indicated in the figures. In **C** and **D**, TNF-α was used to induce insulin resistance in FL83B cells (**C**) and differentiated C2C12 cells (**D**). Control was normal cells without insulin stimulation; control + insulin was normal cells stimulated with insulin; other groups of cells were preincubated for 5 h in medium containing either 10 ng/mL, 20 ng/mL, or 30 ng/mL of TNF-α, as indicated in the figures, then stimulated with insulin. Glucose concentrations of the media were assayed at the time points indicated on the *x*-axis. Glucose concentrations were presented as absorbance at 500 nm and plotted as the *y*-axis. Each experiment was carried out in triplicate. Data represent the mean ± SD. The data set of each cell group was statistically analyzed versus that of the control (in **A** and **B**) or that of control + insulin (in **C** and **D**) by two-way ANOVA. #p between groups <0.05; * p of interaction <0.05.

sensitivity between cultures. This causes inconsistent results between operations or unreliable comparison between experimental groups. In addition, when cell lines were used to analyze insulin-stimulated glucose uptake of cells, radioisotope-labeled (e.g., [³H]-, [¹⁴C]-, or [¹⁸F]-2-deoxy-D-glucose) (*12–14*) or fluorescence-labeled (e.g., 2-NBDG) (*15*) 2-deoxy-glucose is very often used as a glucose analogue to increase the sensitivity of the assay. The safety and handling of radioactive molecules is always a concern, while fluorescence-labeled substitutes and the corresponding supplies for their detection are quite expensive. Thus, the use of either could be problematic in large scale or high-throughput screenings.

To screen and identify hypoglycemic natural products from *M. charantia* that can overcome insulin resistance of cells, we have developed a nonradioactive, nonfluorescent procedure using a normal mouse hepatic cell line FL83B, which does not need differentiation to gain insulin sensitivity. Systematic screening from the stem of *M. charantia* was conducted to identify natural products that can restore glucose uptake of insulin-resistant cells. Moreover, the subcellular actions of these natural products were explored.

MATERIALS AND METHODS

Chemicals and Reagents. Glucose concentration was assayed using Glucose kit (BioSystems, Barcelona, Spain); fetal bovine serum was ordered from Invitrogen (San Diego, USA); bovine insulin solution,

troglitazone, cell culture media, horse serum, mouse TNF-α, DMSO (dimethylsulfoxide), penicillin, streptomycin, and phosphatase inhibitor cocktail 2 were purchased from Sigma Chemical Company (St. Louis, USA).

Extraction, Isolation, and Fractionation of Compounds from *Momordica charantia.* *Momordica charantia* was collected in Pingtung, Taiwan in July, 2003. It was identified by Professor Sheng-Zehn Yang, Department of Forestry, National Pingtung University of Science and Technology. A voucher specimen (no. 2013) has been deposited at the Herbarium of the institution. The isolation procedures of compounds were described previously (*16*). The amounts of CH10, CH63, and CH93 (compounds purified from the extract of *M. charantia* after the screening process, as described in Results) were 10 mg, 6 mg, and 52 mg, respectively, and were isolated from 18 kg bitter melon stems. The partition fractions were evaporated in vacuo to remove the solvent. The resulting residue was dissolved in DMSO in a concentration of 100 mg/mL or 50 mg/mL. Each pure compound (CH10, CH63, CH93) was dissolved in DMSO in 5 mg/mL. When used in the glucose uptake assay, each of these stocks was diluted at least 200-fold into the culture medium of cells to keep the final concentration of DMSO in the medium <0.5%.

Cell Culture and Glucose Uptake Assay. FL83B cells and C2C12 cells were purchased from the American type Culture Collection (Rockville, Maryland, USA). FL83B cells (*17*) were cultured in F12K medium containing 10% fetal bovine serum, 100 units/mL penicillin, and 100 μg/mL streptomycin; C2C12 cells were cultured in DMEM (Dulbecco's modified Eagle's medium) containing 10% fetal bovine serum, 100 units/mL penicillin, and 100 μg/mL streptomycin. Both cells were incubated at 37 °C in a humidified incubator supplied with 5% CO_2.

For the development of insulin resistance by TNF-α, FL83B cells were seeded in 12-well plates at a density of 1×10^4 cells/well and grown for 48 h to reach 80–100% confluence. C2C12 cells were seeded in 12-well plates at a density of 1×10^4 cells/well and grown for 24 h to reach 50% confluence, followed by differentiation in DMEM containing 10% horse serum for 72 h. Both cells were then incubated for 5 h in serum-free medium containing TNF-α.

For the glucose uptake assay, TNF-α-treated cells were incubated for 2 h in serum-free media containing the agent under test. Meanwhile, as control groups, normal and TNF-α-treated cells were incubated for 2 h in serum-free media containing DMSO in a concentration equivalent to that contained in the test group. The media were then replaced with 0.5 mL of MEM (Eagle's minimum essential medium) containing 10% serum, the agent under test, and insulin. Subsequently, at time = 0, 1, 2, 3, 4, and 5 h, 30 μL of the medium was withdrawn and centrifuged at 500*g* for 5 min. Five microliters of the resulting supernatant was mixed with 250 μL of Glucose kit in a 96-well plate and incubated at 37 °C for 10 min. Absorbance at 500 nm was then measured using a microplate reader (Molecular Devices, Sunnyvale, California, USA). The concentration of glucose is in direct proportion to the absorbance.

Statistical Analysis. Data set of cellular glucose uptake was analyzed by two-way analysis of variance (ANOVA), with cell treatment and time (i.e., time points at which medium glucose concentration was measured) as the two parameters. Significance was considered when the p value between groups of cells and the p value of interaction between the two parameters were both <0.05.

Cytotoxicity Assay. Cells were grown in 12-well plates and treated by CH10, CH63, or CH93 as described in the text. The experiment was performed in triplicate. Average percentages of viable cells were determined by trypan blue exclusion assay as described previously (*18*).

Immunoprecipitation and Western Blot Analysis. Cells were washed twice with PBS (phosphate-buffered saline, pH 7.4), submerged in Cell Culture Lysis Reagent (Promega, Madison, Wisconsin, USA) containing phosphatase inhibitor mix (10 mM NaF, 1 mM sodium orthovanadate, 10 mM sodium pyrophosphate; for AMPK), or 1% phosphatase inhibitor cocktail 2 (for IRS-1), and scraped off the plate on ice. The resulting suspension was centrifuged at 4 °C either at 14000*g* for 5 min (for AMPK), or at 500*g* for 1 min (for IRS-1). The

Screening for Compounds Overcoming Insulin Resistance

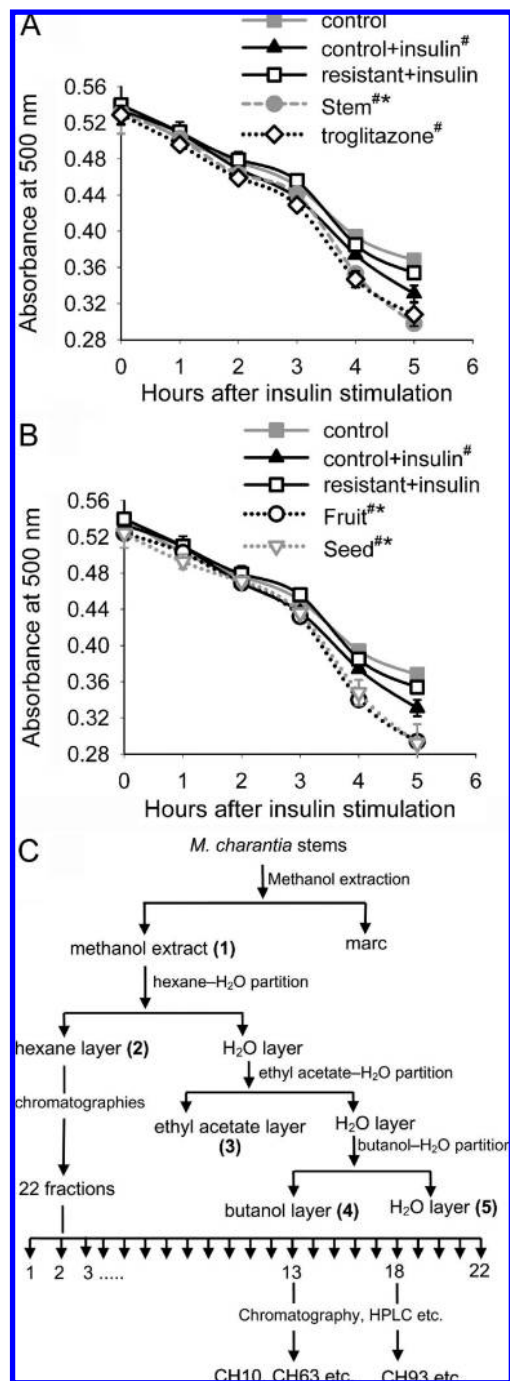*J. Agric. Food Chem.,* Vol. 56, No. 16, 2008 **6837**

Figure 2. Glucose uptake assays for cells treated with the crude extracts from different parts of *M. charantia* and the procedure of the followed partitioning. **A** and **B**, glucose uptake assays as in **Figure 1C**. The treatment of control and control + insulin was identical to that in **Figure 1C**. Resistant + insulin was cells incubated in 20 ng/mL of TNF-α for 5 h (i.e., insulin-resistant cells) before stimulation by insulin. Other groups of cells were insulin-resistant cells treated with 50 μg/mL of the methanol extract of either the stem, fruit, or seed of *M. charantia*, or treated with 50 μM troglitazone, as indicated in the figures, then stimulated by insulin. All groups of cells were assayed simultaneously, but due to the overlapping of curves, crude extract-treated groups were presented separately in two figures to make their curves more observable. The assays were carried out in duplicates. Data represent the mean ± SD. The data set of each group was statistically analyzed versus that of resistant + insulin by two-way ANOVA. #p between groups <0.05; * p of interaction <0.05. C, a flowchart showing the partitioning of the methanol extract of the stem of *M. charantia*.

supernatant was collected and protein concentration was analyzed using the Bradford assay reagent (Bio-Rad, USA).

For the analysis of AMPK, 30 μg of proteins from the supernatant was sampled, electrophoretically fractionated on a 12% polyacrylamide gel, transferred to a PVDF membrane (Amersham Biosciences, UK), and analyzed by Western blotting using an AMPK phosphorylated form (Thr-172)-specific antibody (Cell Signaling Technology, Beverly, Massachusetts, USA), or a β-actin-specific antibody (Chemicon, Temecula, California, USA), as described previously (*18*).

For the analysis of IRS-1, 500 μg of proteins from the supernatant was sampled, mixed with an IRS-1-specific antibody (Cell Signaling Technology) and incubated at 4 °C for 1 h, followed by the addition of Protein G-PLUS agarose (sc-2002, Santa Cruz Biotechnologies, Santa Cruz, California, USA) and incubation at 4 °C for 1 h. After centrifugation at 500*g* for 1 min at 4 °C, the pellet was collected, washed twice with PBS containing 1% phosphatase inhibitor cocktail 2, and resuspended in SDS/PAGE sample buffer. The suspension was heated at 95 °C for 5 min then centrifuged at 500*g* for 5 min to remove insoluble materials. The supernatant was electrophoretically fractionated on a 12% polyacrylamide gel, transferred to a PVDF membrane, and analyzed by Western blotting using a phosphotyrosine-specific antibody (Upstate, Temecula, California, USA), or the IRS-1-specific antibody.

RESULTS

Insulin Sensitivity and Development of Insulin Resistance of FL83B Cells and C2C12 Cells. First, the insulin sensitivity and glucose uptake of FL83B cells was characterized. Insulin was added to the medium to reach 50, 100, or 500 nM. An aliquot of the culture medium was withdrawn for the glucose concentration assay at time interval = 0, 1, 2, 3, 4, and 5 h after the addition of insulin. As depicted in **Figure 1A**, the decline in medium glucose concentration (presented as the absorbance at 500 nm) of control (cells that were not stimulated by insulin) during the 0 to 5 h revealed the rate of glucose uptake by unstimulated cells. Cells incubated in either 50, 100, or 500 nM insulin all showed obviously higher rates of glucose uptake than the control cells did (judged by both p between groups <0.05 and p of interaction <0.05 versus the control by two-way ANOVA) because their medium glucose concentrations declined even faster. One hundred nanomolars of insulin was considered effective enough at promoting glucose uptake of FL83B cells and was chosen to be used in the subsequent experiments.

Meanwhile, the same characterization was performed for differentiated C2C12 cells for comparison. On the basis of previous reports, 100 nM and 1 μM of insulin were tried on C2C12 cells. As shown in **Figure 1B**, the effect of 100 nM insulin on increasing glucose uptake of the cell was less obvious, and that of 1 μM insulin was more satisfactory (judged by both p between groups <0.05 and p of interaction <0.05 versus the control by two-way ANOVA). Thus, 1 μM insulin was used in the subsequent experiments for C2C12 cells.

Tumor necrosis factor-α (TNF-α) has been suggested to be an important factor for the development of insulin resistance physiologically because most type 2 diabetic patients have increased TNF-α expression from adipose tissues (*19*). Moreover, TNF-α was shown to cause insulin resistance in muscle cells (*13*) and adipocytes (*20*). Thus, to mimic the physiological conditions that lead to the development of insulin resistance in tissues, we tried to induce insulin resistance in FL83B cells by TNF-α.

FL83B cells were treated with TNF-α for 5 h, then incubated in serum-free medium for 2 more hours. Subsequently, the cells were stimulated by 100 nM insulin, followed by the medium glucose concentration assay at time interval = 0, 1, 2, 3, 4, and 5 h after the addition of insulin. As depicted in **Figure 1C**,
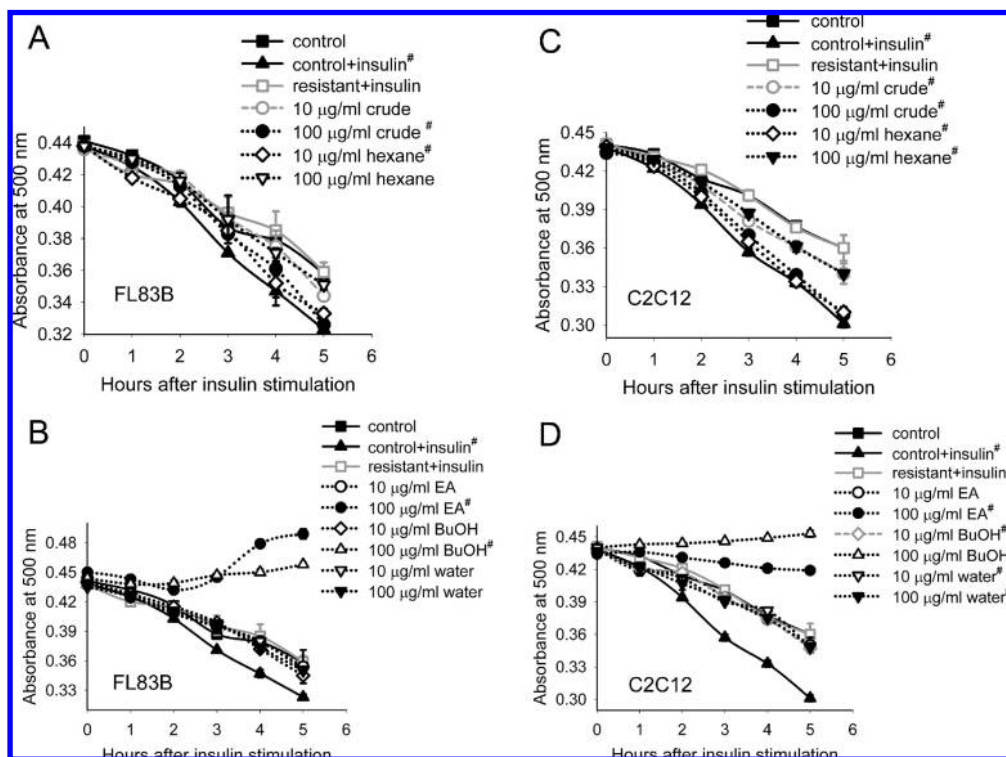
Figure 3. Glucose uptake assays for cells treated with the partitions of the methanol extract of bitter melon stems. Glucose uptake assays were performed as in **Figure 2**. **A** and **B**, FL83B cells; **C** and **D**, differentiated C2C12 cells. Crude, hexane, EA (ethyl acetate), BuOH (butanol), and water represent insulin-resistant cells treated with the partition marked as (1), (2), (3), (4), and (5) in **Figure 2C**, respectively, then stimulated with insulin. The assays were carried out in triplicate. Data represent the mean ± SD. The data set of each group was statistically analyzed versus that of resistant + insulin by two-way ANOVA. [#]*p* between groups and *p* of interaction both <0.05.

control was cells neither treated by TNF-α nor stimulated by insulin; control + insulin was cells not pretreated by TNF-α but stimulated with 100 nM insulin. This group of cells showed an obviously higher rate of glucose uptake than the control did (*p* between groups and *p* of interaction both <0.05 control versus control + insulin). However, when cells were pretreated with 10 or 20 ng/mL of TNF-α before stimulation by 100 nM of insulin, their rates of glucose uptake were both significantly reduced as compared to that of control + insulin (**Figure 1C**, both were *p* between groups <0.05 and *p* of interaction <0.05 versus control + insulin) and were similar to that of the control. It indicated that insulin sensitivity was lost or insulin resistance was developed in these cells. The effect of 20 ng/mL of TNF-α was considered more obvious and thus was chosen to develop insulin resistance in FL83B cells in the subsequent experiments.

Simultaneously, the same assay was performed for differentiated C2C12 cells. As shown in **Figure 1D**, pretreatment by either 10, 20, or 30 ng/mL of TNF-α all resulted in an apparent decline of insulin-stimulated glucose uptake in these cells compared to control + insulin (*p* between groups and *p* of interaction both <0.05 versus control + insulin), and their rates of glucose uptake were similar to that of the control. The effect of 30 ng/mL of TNF-α was considered most obvious and thus was used for C2C12 cells in the subsequent experiments.

Tests of the Hypoglycemic Effects of the Crude Extracts from Different Parts of *M. charantia in Vitro.* The hypoglycemic effects of methanol extracts from the fruit, seed, and stem of *M. charantia* were tested using insulin-resistant FL83B cells *in vitro*. In **Figure 2A** and **B**, the treatments for cells of control and control + insulin were identical to those in **Figure 1C**, while insulin-resistant cells (cells pretreated with 20 ng/mL of TNF-α) stimulated by insulin were plotted as resistant + insulin. When insulin-resistant FL83B cells were incubated for 2 h

before insulin stimulation in 50 μg/mL of methanol extract from the fruit, seed, or stem of *M. charantia*, they all showed elevated glucose uptake when compared to resistant + insulin (*p* between groups and *p* of interaction both <0.05 versus resistant + insulin), and their glucose uptake was higher than that of control + insulin (**Figure 2A** and **B**). For comparison, the effect of an antidiabetic agent, troglitazone, a thiazolidinedione type medicine used to treat insulin resistance clinically (*21*), was tested simultaneously. Troglitazone (50 μM, or 22 μg/mL) displayed an effect similar to that of the bitter melon extracts (**Figure 2A**). These data revealed that the extracts from the fruit, seed, or stem of bitter melon all contained components efficacious in improving glucose uptake of insulin-resistant cells.

Further Partitioning and Characterization of the Methanol Extract of Bitter Melon Stems. Components in the methanol extract of the stem of *M. charantia* were further partitioned stepwise based on their polarities (*16*). Briefly, methanol was removed by evaporation. The residue was dissolved in H_2O and partitioned sequentially with hexane, ethyl acetate (EA), then butanol (**Figure 2C**). Aliquots from the methanol extract, hexane, EA, and butanol layers, and final water layer [**Figure 2C**, marked as (1), (2), (3), (4), and (5), respectively] were vacuum-dried and dissolved in DMSO for the following tests.

The effects of these partitions on cellular glucose uptake were tested in insulin-resistant FL83B cells. Cells were incubated in 10 or 100 μg/mL of each partition, and insulin-stimulated glucose uptake was then assayed as in **Figure 2**. Consequently, 100 μg/mL of methanol extract and 10 μg/mL of hexane layer showed significant effects on promoting glucose uptake of insulin-resistant cells (**Figure 3A**) judged by *p* between groups and *p* of interaction both <0.05 versus resistant + insulin, plus a rate of glucose uptake close to that of control + insulin. The
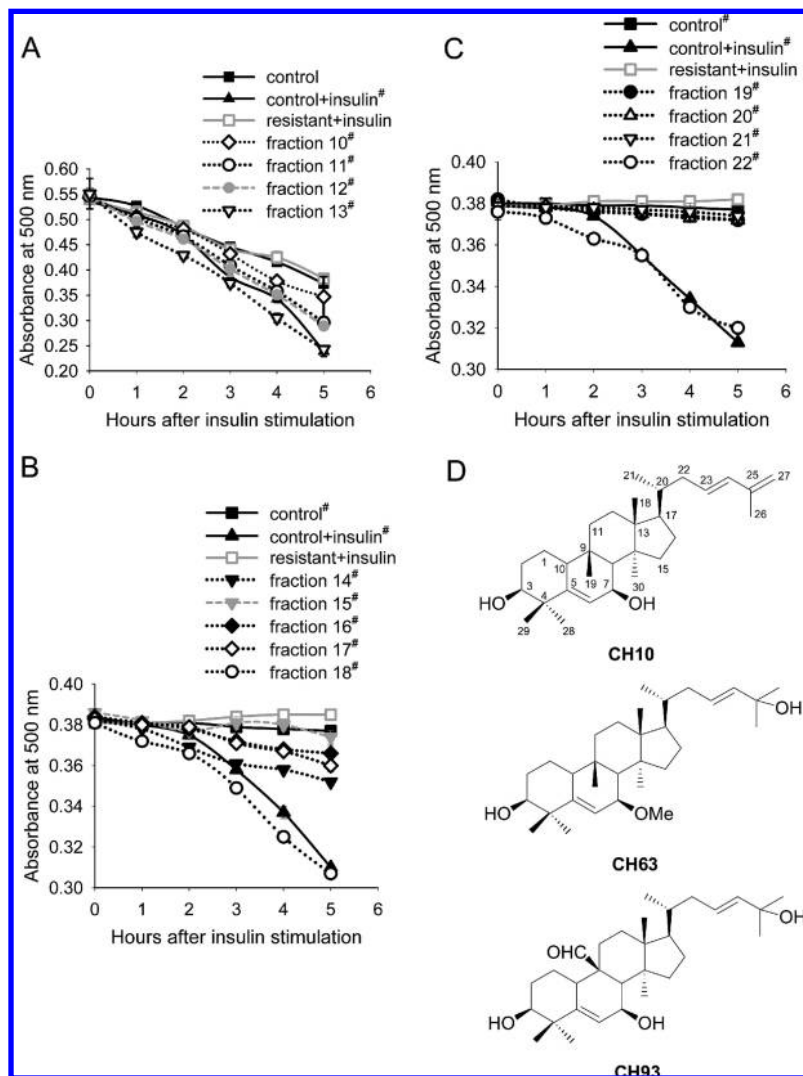
Screening for Compounds Overcoming Insulin Resistance

J. Agric. Food Chem., Vol. 56, No. 16, 2008   **6839**

Figure 4. Glucose uptake assays for cells treated with the fractions of hexane layer and the structures of CH10, CH63, and CH93. **A**, assays for fractions 10−13; **B**, assays for fractions 14−18; **C**, assays for fractions 19−22. All fractions were in 10 μg/mL, and all were performed in FL83B cells in triplicate. Data represent the mean $\pm$ SD. The data set of each group was statistically analyzed versus that of resistant + insulin by two-way ANOVA. [#]*p* between groups and *p* of interaction both <0.05. **D**, the chemical structures of CH10, CH63, and CH93.

methanol extract in a lower concentration (10 μg/mL) was less effective. On the contrary, the effectiveness of the hexane layer was reduced when used in a higher concentration (100 μg/mL; **Figure 3A**), indicating an upper limit for the effective dosage. Other partitions (**Figure 3B**) showed either no effects or inhibitory effects (100 μg/mL of EA layer and 100 μg/mL of butanol layer) on glucose uptake. It suggested that compounds in the methanol extract that could improve glucose uptake of insulin-resistant cells were distributed into the hexane layer during the partition. To inspect whether these results observed in FL83B cells were repeatable in another type of insulin-sensitive cells, the same tests were carried out in insulin-resistant C2C12 cells, and similar results were obtained (**Figure 3C** and **D**).

Screening for Constituents Improving Cellular Insulin Resistance from the Hexane Layer. Materials in the hexane layer were further split into 22 fractions by column chromatography, HPLC, and so forth (**Figure 2C**) (*16*), and each fraction was tested using insulin-resistant FL83B cells. To select the most active fractions, in addition to *p* between groups and *p* of interaction both <0.05 versus resistant + insulin by two-way ANOVA, only those with a rate of glucose uptake overlapping with or even higher than that of control + insulin

were considered. Consequently, three of them, fractions 13, 18, and 22, showed the most obvious activities on restoring the glucose uptake of insulin-resistant cells to the level of control + insulin. The results of fractions 10 to 22 are illustrated in **Figure 4A−C**.

The constituents of fractions 13 and 18 have been further purified (*16*), which afforded 7 compounds (all triterpenes) from fraction 13 and 5 (1 triterpene, 3 steroids, and 1 aromatic compound) from fraction 18 for identification. The two major ones of fraction 13 are (23*E*)-cucurbita-5,23,25-triene-3β,7β-diol (designated as CH10) (*16*) and 3β,25-dihydroxy-7β-methoxycucurbita-5,23(*E*)-diene (designated as CH63) (*11*); the major compound identified from fraction 18 is 3β,7β,25-trihydroxycucurbita-5,23(*E*)-dien-19-al (designated as CH93) (*22*), the only triterpene in this fraction. The structures of CH10, CH63, and CH93 are shown in **Figure 4D**.

The effects of 10 μg/mL of CH10, CH63, and CH93 were tested in insulin-resistant FL83B cells. As illustrated in **Figure 5A**, each of them showed an effect on promoting glucose uptake of insulin-resistant FL83B cells to the level of control + insulin.

The above glucose uptake assays for the effects of bitter melon extracts, fractions, or single compounds were done by preincubating insulin-resistant cells in the extracts or compounds
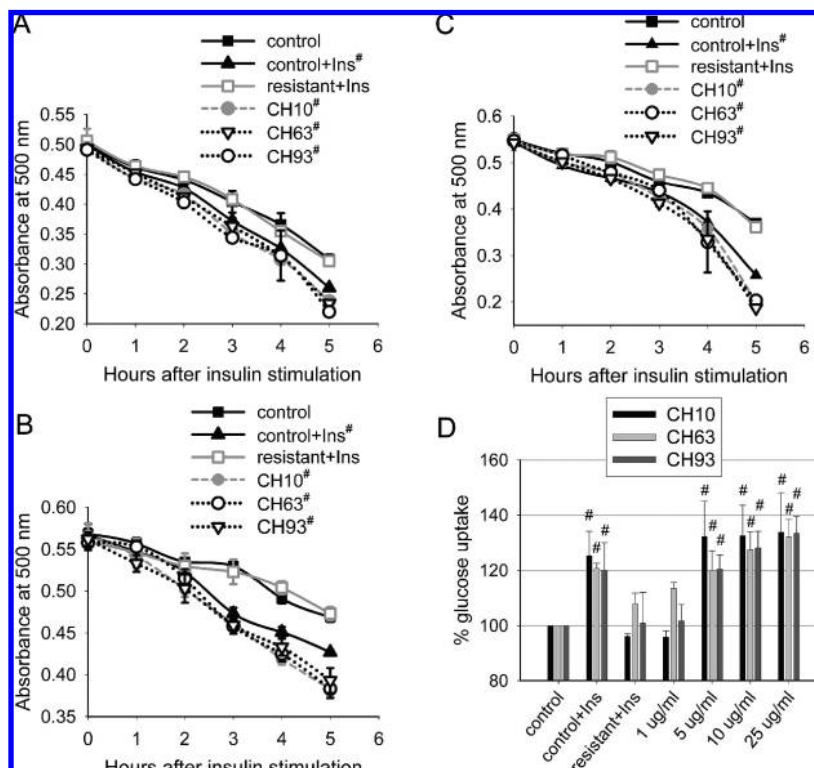
Figure 5. Glucose uptake assays for cells treated with CH10, CH63, or CH93. Ins, insulin. In **A**, the handling of cells was identical to that in **Figures 2–4**; in **B**–**D**, the 2-h preincubation of cells in the compound (CH10, CH63, or CH93) or in a serum-free medium (the control groups) before insulin stimulation, was omitted. **C** was performed in C2C12 cells; others were performed in FL83B cells. In **A**–**C**, CH10, CH63, and CH93 were used in 10 μg/mL. **D**, to observe dosage dependence, different concentrations of CH10, CH63, and CH93 were tested as indicated in the *x*-axis. The assay was performed as in **B**, but the total amount of medium glucose consumed by each cell group between 0 and 5 h of insulin stimulation was calculated and plotted as % glucose uptake versus control in the *y*-axis. All assays were performed in triplicate. Data represent the mean $\pm$ SD. The data set of each group was analyzed by two-way ANOVA versus resistant + insulin. [#]p between groups and p of interaction both <0.05 versus resistant + insulin.

for 2 h before insulin stimulation. It was examined next whether these compounds are effective if the 2-h preincubation is skipped. Thus, CH10, CH63, or CH93 was added to the medium of insulin-resistant FL83B cells together with insulin, immediately followed by the glucose uptake assay. The results exhibited that these compounds were still able to promote the glucose uptake of insulin-resistant cells to the level of control + insulin (**Figure 5B**). The same test was also performed in insulin-resistant C2C12 cells, and similar results were obtained (**Figure 5C**). Thus, the 2-h preincubation of cells in these compounds was omitted in the following experiments.

The dosage dependence of CH10, CH63, and CH93 was characterized subsequently. The activities of these compounds in 1, 5, 10, and 25 μg/mL were tested. Consequently, dosage dependence was observed in all cases (**Figure 5D**). In each case, 5 μg/mL, 10 μg/mL, and 25 μg/mL were effective, while 1 μg/mL had no effect as revealed statistically.

The cytotoxicity of CH10, CH63, and CH93 was analyzed next. FL83B cells or C2C12 cells were incubated in 10 or 50 μg/mL of Ch10, CH63, or CH93 for 7 h (the time length of cells incubated in the compounds in **Figure 5A**). In 10 μg/mL, the average percentages of viable FL83B cells relative to the control (FL83B cells incubated in 1% DMSO) were 98.6%, 98.2%, and 98.7% for CH10, CH63, and CH93, respectively. In 50 μg/mL, those of viable FL83B cells relative to the control were 95.7%, 96.1%, and 95.3% for CH10, CH63, and CH93, respectively. For C2C12 cells, the average percentages of viable cells versus the control (C2C12 cells incubated in 1% DMSO)

were 93.8%, 98.2%, and 110.6% for 50 μg/mL of CH10, CH63, and CH93, respectively. Thus, no obvious cytotoxicity was observed for these compounds under these concentrations.

Characterization of the Subcellular Actions of CH10, CH63, and CH93. The effects of CH10, CH63, and CH93 in ameliorating insulin resistance were checked subcellularly by examining the level of IRS-1 tyrosine phosphorylation. Following the activation of insulin receptor by the association with insulin, the tyrosine phosphorylation of insulin receptor substrate (IRS) occurs, which activates the insulin signaling pathway. IRS-1 is one of the two major isoforms of IRS in hepatocytes. As shown in **Figure 6A**, immunoprecipitation of IRS-1 followed by Western blotting with a phosphotyrosine-specific antibody (panel Y–P) revealed that the level of IRS-1 tyrosine phosphorylation in insulin-stimulated normal FL83B cells (control + insulin) was indeed higher than that of unstimulated cells (control). Nonetheless, when insulin-resistant cells were stimulated with insulin (resistant + insulin), their level of IRS-1 tyrosine phosphorylation was similar to or even lower than that of the control. Consistently, these results can be observed in **Figure 6B** and **C** as well. When insulin-resistant cells were incubated in either CH10-, CH63-, CH93-, or troglitazone-containing medium and simultaneously stimulated with insulin (**Figure 6A**), their levels of IRS-1 tyrosine phosphorylation were all elevated to be higher than those of the control and resistant + insulin. The effects of CH10 and CH93 were more obvious; thus, the experiment was repeated for CH10 (**Figure 6B**) and CH93 (**Figure 6C**). Meanwhile, the effect of the hexane layer was also tested (**Figure 6C**). Again, the level of IRS-1 tyrosine
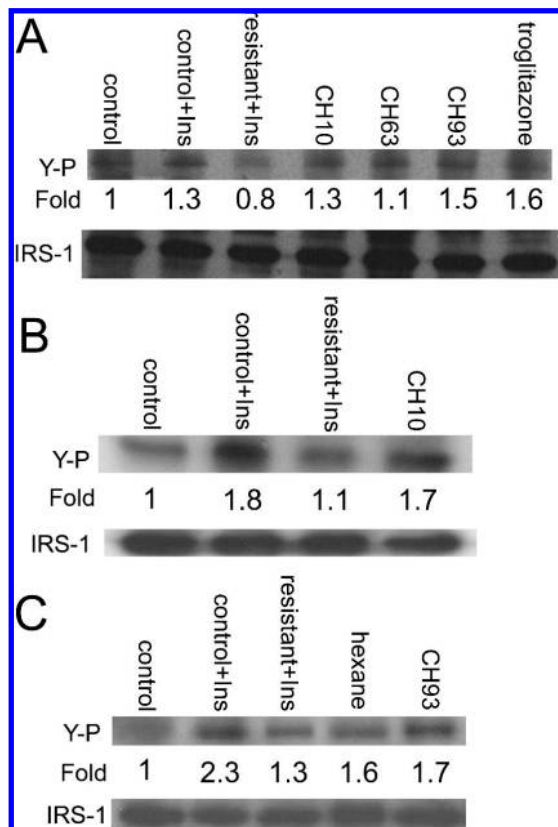
Screening for Compounds Overcoming Insulin Resistance

J. Agric. Food Chem., Vol. 56, No. 16, 2008 **6841**

Figure 6. Detection of IRS-1 tyrosine phosphorylation in FL83B cells by Western blotting. Ins, insulin. The handling of control, control + Ins, and resistant + Ins was identical to that in **Figure 5B**−**D**. **A**, lanes CH10, CH 63, CH93, and troglitazone were insulin-resistant cells stimulated by insulin and incubated in 10 μg/mL of CH10, CH 63, or CH93, or in 50 μM troglitazone, respectively. Cells were harvested at 30 min after insulin stimulation. Cellular proteins were immunoprecipitated by an IRS-1-specific antibody, then analyzed by Western blotting using either a phosphotyrosine-specific antibody (panel Y−P), or the IRS-1-specific antibody (panel IRS-1). It was a single experiment. **B**, the test was repeated once for CH10. **C**, the test was repeated once for CH93, and the effect of 10 μg/mL of hexane layer (lane hexane) was compared. Fold represents the relative band intensities between lanes in panel Y−P that were prenormalized by the amount of IRS-1 (as revealed in panel IRS-1). The band intensity of the control was set as 1.

phosphorylation in CH10-treated cells (**Figure 6B**, lane CH10), in CH93-treated cells (**Figure 6C**, lane CH93), or in hexane layer-treated cells (**Figure 6C**, lane hexane) was elevated as compared to those of the control and resistant + insulin. These data supported an effect of these compounds on overcoming cellular insulin resistance and reactivating the insulin signaling pathway.

It was proposed that the hypoglycemic effect of bitter melon might be mediated by AMPK (AMP-activated protein kinase) (*23*). Furthermore, AMPK is suggested to be able to increase the tyrosine phosphorylation of IRS-1 (*24*). Hence, whether CH10, CH63, or CH93 could activate AMPK in FL83B cells was examined. Because AMPK is known to be activated by phosphorylation at Thr-172 of the α subunit (*25*), an antibody specific for the Thr-172 phosphorylated form of AMPK was used for the assay. As shown in **Figure 7A**, the phosphorylation of AMPK was increased in control + insulin and reduced in resistant + insulin as compared to that of the control. Whereas in cells treated with CH10, CH63, CH93, or the methanol extract (crude), the phosphorylation of AMPK was apparently elevated as compared to that of resistant + insulin and of the control

and even higher than that of control + insulin (**Figure 7A**, lanes CH10, CH63, CH93, and crude). This suggests the activation of AMPK by these compounds.

Furthermore, when cells were harvested at different time points (0, 10, 30, 60 min and 5 h after the addition of insulin), the phosphorylation level of AMPK was shown to be steady but slightly declined in the control and in resistant + insulin during the time course (**Figure 7B** and **C**), though it was increased in resistant + insulin at 5 h. In control + insulin, the addition of insulin resulted in slightly elevated phosphorylation of AMPK (less than 1.5-fold; **Figure 7B** and **C**). When insulin-resistant cells were treated with either CH10, CH63, or CH93, the phosphorylation of AMPK was apparently raised during the whole time and peaked at 30 min (over 3-fold in CH10- or CH93-treated cells; **Figure 7B** and **C**). These findings again strongly suggested that AMPK was activated by CH10, CH63, and CH93 in the treated cells.

DISCUSSION

This report was the first to demonstrate a systematic screening and identification of potential hypoglycemic molecules in the stem of *M. charantia* according to their abilities in overcoming cellular insulin resistance. The results suggest that triterpenoids in the extract of bitter melon stems have a high potential for hypoglycemic activities, and their actions are likely mediated by the activation of AMPK. Meanwhile, a new strategy without the use of fluorescent or radioisotope-labeled glucose analogues was illustrated to efficiently monitor cellular glucose uptake and screen for hypoglycemic molecules.

New Strategy for the Screening of Hypoglycemic Agents and the Analysis of Cellular Glucose Uptake. It was shown in this study that the glucose uptake of a normal liver cell line, FL83B, was enhanced by the stimulation of insulin. Furthermore, FL83B cells showed higher insulin sensitivity than the myocyte C2C12 cells did. The mechanism underlying these phenomena needs further characterization. The advantage of FL83B cells over muscle cell lines and adipocytes is that it needs no further differentiation for the assay. This largely reduces the complexity of the operation. Moreover, results obtained from FL83B cells and from C2C12 cells were consistent whenever examined in this study. Thus, using FL83B cells to replace the commonly used muscle or adipose cell lines offers the development of a cell-based screening system for hypoglycemic molecules.

Because of the inherent sensitivity of radioactivity and fluorescence measurements, cellular glucose uptake has often been detected by supplying radioactive or fluorescent substitutes of glucose in the medium. These methods are highly sensitive but could suffer from background interference. Nonetheless, a nonradioactive and cost-effective method was demonstrated in this study. The method afforded a screening from a complicated source for potential hypoglycemic molecules that are effective for insulin-resistant cells. Additionally, the method did not involve filtration, separation, or wash of cells in the steps, which are necessary for radioactive or fluorescent methods and can be time-consuming and difficult for automation.

Screening and Identification of Potential Hypoglycemic Components in the Stem of *M. charantia*. In most previous studies, the crude water, ethanol, or methanol extract of *M. charantia* (mostly from the fruit of the plant) was used to test for a hypoglycemic effect in chemically induced (*7, 26*) or genetic models (*27*) of diabetic animals. However, few have characterized the active components in the extracts responsible for the action. Although a few phytochemicals, including
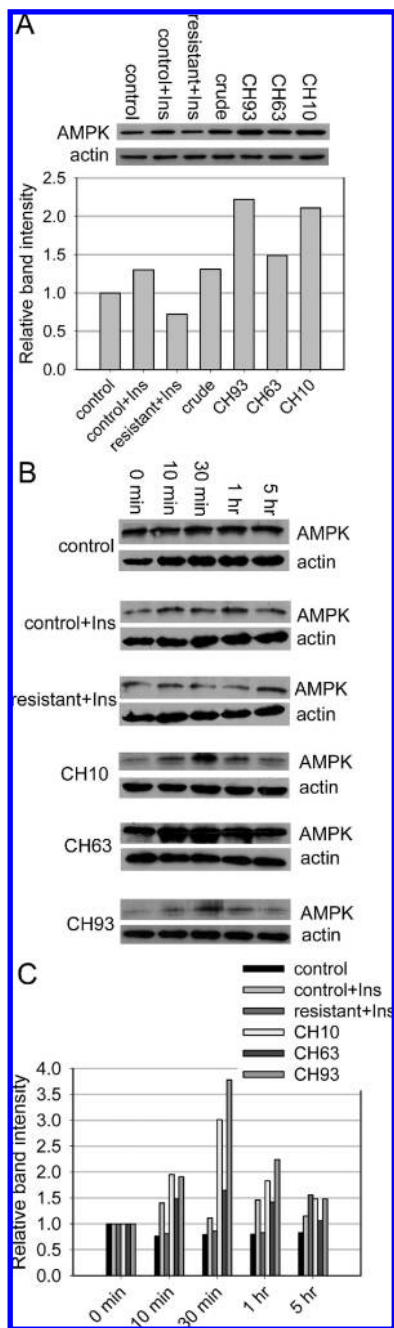
Figure 7. Western blot analysis for AMPK phosphorylation in FL83B cells. Cells were processed as in **Figure 5B** and analyzed by Western blotting using an antibody specific for the phosphorylated form of AMPK (panel AMPK) and an antibody for β-actin (panel actin). Ins, insulin. **A**, the comparison of control, control + insulin, and resistant + insulin with cells treated with the methanol extract of the stem of *M. charantia* (crude, 50 μg/mL), CH93, CH63, or CH10 (each in 10 μg/mL). Cells were harvested at 30 min after insulin stimulation. It was a single experiment. The histogram shows the relative band intensities of phosphorylated AMPK that were normalized by the levels of actin, with the band intensity of the control being set as 1. **B**, control, control + Ins, resistant + Ins, CH10-treated, CH63-treated, and CH93-treated cells were harvested at 0 min, 10 min, 30 min, 1 h, and 5 h after insulin stimulation and analyzed by Western blotting using the antibody specific for phosphorylated AMPK. Each was a single experiment. **C**, a histogram showing the relative band intensities of phosphorylated AMPK of the data presented in **B**. Data were normalized by the levels of actin, and the band intensity of time = 0 min was set as 1 in each group.

charantin, polypeptide-p, momordin Ic, oleanolic acid 3-*O*-monodesmoside, oleanolic acid 3-*O*-glucuronide, and triterpenoids, and so forth, were isolated in a stochastic and sporadic manner from the fruit of *M. charantia* and tested in animals for hypoglycemic activities (*9–11*). Even less analyzed were the effects of the extracts or phytochemicals on insulin resistance at the organism or cellular level because most of the experimental animals used were not exactly insulin-resistant models.

The data shown here revealed that the fruit, seed, and stem of *M. charantia* contained ingredients with the ability to overcome cellular insulin resistance and restore glucose uptake of cells. These ingredients in the crude extract of the stem of *M. charantia* were systematically screened, and 3 out of 22 fractions (fractions 13, 18, and 22) were considered to be most active. The main constituents identified from fractions 13 and 18 were triterpenoids CH10, CH63, and CH93. They were subsequently confirmed as being able to overcome cellular insulin resistance, as manifested by the recovery of glucose uptake and IRS-1 tyrosine phosphorylation in insulin-resistant cells. Coincidentally, CH93 was stochastically isolated previously from the fruit of *M. charantia* by another group and was shown to have an acute hypoglycemic effect when tested in alloxan-induced diabetic mice (*11*). This provides evidence for the hypoglycemic activity of this compound *in vivo*. Overall, these results strongly suggest triterpenoids to be one important type of hypoglycemic molecules in the stem of *M. charantia*. Meanwhile, CH93 and CH63 were also previously isolated from the fruit of *M. charantia* by other groups (*11, 22*). Thus, it is very likely that different parts of *M. charantia* contain overlapping hypoglycemic molecules.

Meanwhile, it was observed that EA and BuOH layers in a higher concentration (100 μg/mL) caused an apparent inhibiting effect on glucose uptake in both FL83B and C2C12 cells (**Figure 3B** and **D**). Their medium glucose levels were even higher than that of the control. This implied that the regular cell physiology for glucose metabolism in FL83B and C2C12 cells might be disturbed by EA and BuOH layers at higher concentrations. Components causing this effect in EA and BuOH layers are not clear. Nonetheless, this might also explain why the hexane layer was less active when used in a higher concentration (100 μg/mL) in both FL83B and C2C12 cells (**Figure 3A** and **C**). It is likely that the hexane layer also contained some inhibitory components causing suppressed glucose uptake as those in EA and BuOH layers. When used in a higher concentration, these inhibitory components crossed a concentration threshold and started to counteract the effects of hypoglycemic compounds, resulting in the observed decline of hypoglycemic effect of the hexane layer. Overall, this indicated that bitter melon also contains some inhibitory components that could disturb cellular glucose uptake.

Subcellular Actions of the *M. charantia* Triterpenoids. Our data suggested that the crude extract, CH10, CH63, and CH93 from the stem of bitter melon all led to the activation of AMPK in cells. Meanwhile, it was also demonstrated that these compounds enhanced the tyrosine phosphorylation of IRS-1 in insulin-resistant cells. Overall, these gave a clue as to the subcellular mechanism of their effects on reducing the insulin resistance of cells. Previous reports showed that AMPK can catalyze the phosphorylation of IRS-1 at Ser-789, which promotes insulin-stimulated tyrosine phosphorylation of IRS-1 (*24*). Thus, it is likely that CH10, CH63, or CH93 activated AMPK, which increased IRS-1 tyrosine phosphorylation that was inhibited by TNF-α, and rebooted the insulin signaling pathway.

Screening for Compounds Overcoming Insulin Resistance

J. Agric. Food Chem., Vol. 56, No. 16, 2008 **6843**

Recently, AMPK has been recognized as a potential drug target for the treatment of metabolic diseases including obesity and type 2 diabetes (*28, 29*). It is suggested to be a cellular energy sensor that promotes ATP-production catabolic pathways, including glucose uptake, and suppresses ATP-consuming processes (*29, 30*). However, in FL83B cells, regulation of cellular activities by AMPK and the mechanism controlling glucose uptake, such as glucose transporters, have not been well characterized. Thus, further investigation is required for a complete understanding of the molecular mechanism underlying the actions of *M. charantia* triterpenoids.

ABBREVIATIONS USED

TNF-α, tumor necrosis factor-α; EA, ethyl acetate; IRS, insulin receptor substrate; CH10, (23*E*)-cucurbita-5,23,25-triene-3β,7β-diol; CH63, 3β,25-dihydroxy-7β-methoxycucurbita-5,23(*E*)-diene; CH93, 3β,7β,25-trihydroxycucurbita-5,23(*E*)-dien-19-al; AMPK, AMP-activated protein kinase.

LITERATURE CITED

(1) Kasuga, M. Insulin resistance and pancreatic beta cell failure. *J. Clin. Invest.* **2006**, *116*, 1756–60.

(2) Fujimoto, W. Y. The importance of insulin resistance in the pathogenesis of type 2 diabetes mellitus. *Am. J. Med* **2000**, *108*, 9S–14S.

(3) Lebovitz, H. E.; Banerji, M. A. Treatment of insulin resistance in diabetes mellitus. *Eur. J. Pharmacol.* **2004**, *490*, 135–46.

(4) Eckel, R. H.; Grundy, S. M.; Zimmet, P. Z. The metabolic syndrome. *Lancet* **2005**, *365*, 1415–28.

(5) Kahn, B. B.; Flier, J. S. Obesity and insulin resistance. *J. Clin. Invest.* **2000**, *106*, 473–81.

(6) Grover, J. K.; Yadav, S. P. Pharmacological actions and potential uses of *Momordica charantia*: a review. *J. Ethnopharmacol.* **2004**, *93*, 123–32.

(7) Reyes, B. A.; Bautista, N. D.; Tanquilut, N. C.; Anunciado, R. V.; Leung, A. B.; Sanchez, G. C.; Magtoto, R. L.; Castronuevo, P.; Tsukamura, H.; Maeda, K. I. Anti-diabetic potentials of *Momordica charantia* and *Andrographis paniculata* and their effects on estrous cyclicity of alloxan-induced diabetic rats. *J. Ethnopharmacol.* **2006**, *105*, 196–200.

(8) Donya, A.; Hettiarachchy, N.; Liyanage, R.; Lay, J., Jr.; Chen, P.; Jalaluddin, M. Effects of processing methods on the proximate composition and momordicosides K and L content of bitter melon vegetable. *J. Agric. Food Chem.* **2007**, *55*, 5827–33.

(9) Khanna, P.; Jain, S. C.; Panagariya, A.; Dixit, V. P. Hypoglycemic activity of polypeptide-p from a plant source. *J. Nat. Prod.* **1981**, *44*, 648–55.

(10) Matsuda, H.; Li, Y.; Murakami, T.; Matsumura, N.; Yamahara, J. III Structure-related inhibitory activity and action mode of oleanolic acid glycosides on hypoglycemic activity. *Chem. Pharm. Bull. (Tokyo)* **1998**, *46*, 1399–403.

(11) Harinantenaina, L.; Tanaka, M.; Takaoka, S.; Oda, M.; Mogami, O.; Uchida, M.; Asakawa, Y. *Momordica charantia* constituents and antidiabetic screening of the isolated major compounds. *Chem. Pharm. Bull. (Tokyo)* **2006**, *54*, 1017–21.

(12) Chen, D.; Elmendorf, J. S.; Olson, A. L.; Li, X.; Earp, H. S.; Pessin, J. E. Osmotic shock stimulates GLUT4 translocation in 3T3L1 adipocytes by a novel tyrosine kinase pathway. *J. Biol. Chem.* **1997**, *272*, 27401–10.

(13) del Aguila, L. F.; Claffey, K. P.; Kirwan, J. P. TNF-alpha impairs insulin signaling and insulin stimulation of glucose uptake in C2C12 muscle cells. *Am. J. Physiol.* **1999**, *276*, E849–55.

(14) Yu, Z. W.; Buren, J.; Enerback, S.; Nilsson, E.; Samuelsson, L.; Eriksson, J. W. Insulin can enhance GLUT4 gene expression in 3T3-F442A cells and this effect is mimicked by vanadate but counteracted by cAMP and high glucose-potential implications for insulin resistance. *Biochim. Biophys. Acta* **2001**, *1535*, 174–85.

(15) Yoshioka, K.; Takahashi, H.; Homma, T.; Saito, M.; Oh, K. B.; Nemoto, Y.; Matsuoka, H. A novel fluorescent derivative of glucose applicable to the assessment of glucose uptake activity of *Escherichia coli*. *Biochim. Biophys. Acta* **1996**, *1289*, 5–9.

(16) Chang, C. I.; Chen, C. R.; Liao, Y. W.; Cheng, H. L.; Chen, Y. C.; Chou, C. H. Cucurbitane-type triterpenoids from *Momordica charantia*. *J. Nat. Prod.* **2006**, *69*, 1168–71.

(17) Breslow, J. L.; Sloan, H. R.; Ferrans, V. J.; Anderson, J. L.; Levy, R. I. Characterization of the mouse liver cell line FL83B. *Exp. Cell Res.* **1973**, *78*, 441–53.

(18) Cheng, H. L.; Chang, S. M.; Cheng, Y. W.; Liu, H. J.; Chen, Y. C. Characterization of the activities of p21Cip1/Waf1 promoter-driven reporter systems during camptothecin-induced senescence-like state of BHK-21 cells. *Mol. Cell. Biochem.* **2006**, *291*, 29–38.

(19) Hotamisligil, G. S.; Shargill, N. S.; Spiegelman, B. M. Adipose expression of tumor necrosis factor-alpha: direct role in obesity-linked insulin resistance. *Science* **1993**, *259*, 87–91.

(20) Iwata, M.; Haruta, T.; Usui, I.; Takata, Y.; Takano, A.; Uno, T.; Kawahara, J.; Ueno, E.; Sasaoka, T.; Ishibashi, O.; Kobayashi, M. Pioglitazone ameliorates tumor necrosis factor-alpha-induced insulin resistance by a mechanism independent of adipogenic activity of peroxisome proliferators-activated receptor-gamma. *Diabetes* **2001**, *50*, 1083–92.

(21) Rangwala, S. M.; Lazar, M. A. Peroxisome proliferator-activated receptor gamma in diabetes and metabolism. *Trends Pharmacol. Sci.* **2004**, *25*, 331–6.

(22) Fatope, M. O.; Takeda, Y.; Yamashita, H.; Okabe, H.; Yamauchi, T. New cucurbitane triterpenoids from *Momordica charantia*. *J. Nat. Prod.* **1990**, *53*, 1491–1497.

(23) McCarty, M. F. Does bitter melon contain an activator of AMP-activated kinase. *Med. Hypotheses* **2004**, *63*, 340–3.

(24) Jakobsen, S. N.; Hardie, D. G.; Morrice, N.; Tornqvist, H. E. 5′-AMP-activated protein kinase phosphorylates IRS-1 on Ser-789 in mouse C2C12 myotubes in response to 5-aminoimidazole-4-carboxamide riboside. *J. Biol. Chem.* **2001**, *276*, 46912–6.

(25) Hawley, S. A.; Davison, M.; Woods, A.; Davies, S. P.; Beri, R. K.; Carling, D.; Hardie, D. G. Characterization of the AMP-activated protein kinase kinase from rat liver and identification of threonine 172 as the major site at which it phosphorylates AMP-activated protein kinase. *J. Biol. Chem.* **1996**, *271*, 27879–87.

(26) Sarkar, S.; Pranava, M.; Marita, R. Demonstration of the hypoglycemic action of *Momordica charantia* in a validated animal model of diabetes. *Pharmacol. Res.* **1996**, *33*, 1–4.

(27) Miura, T.; Itoh, C.; Iwamoto, N.; Kato, M.; Kawai, M.; Park, S. R.; Suzuki, I. Hypoglycemic activity of the fruit of the *Momordica charantia* in type 2 diabetic mice. *J. Nutr. Sci. Vitaminol. (Tokyo)* **2001**, *47*, 340–4.

(28) Hardie, D. G. The AMP-activated protein kinase pathway-new players upstream and downstream. *J. Cell Sci.* **2004**, *117*, 5479–87.

(29) Long, Y. C.; Zierath, J. R. AMP-activated protein kinase signaling in metabolic regulation. *J. Clin. Invest.* **2006**, *116*, 1776–83.

(30) Du, M.; Shen, Q. W.; Zhu, M. J. Role of beta-adrenoceptor signaling and AMP-activated protein kinase in glycolysis of postmortem skeletal muscle. *J. Agric. Food Chem.* **2005**, *53*, 3235–9.